JOURNAL OF MATERIALS SCIENCE 20 (1985) 1961–1975

The crystal growth of silicon in Al–Si alloys

K. F. KOBAYASHI*, L. M. HOGAN
Department of Mining and Metallurgical Engineering, University of Queensland, St Lucia, Queensland 4067, Australia

Some crystallographic observations of primary silicon and unmodified eutectic silicon in aluminium–silicon alloys are summarized and used to support the theory that sodium modification is due to the poisoning of active growth centres. The implications of endogenous growth in unmodified aluminium–silicon sand castings are explored and mechanisms are proposed for the flake–fibre transition in chill-modified and sodium-modified alloys.

1. Introduction

The remarkable variety of morphologies exhibited by silicon crystals in Al–Si alloys has inspired a long series of research investigations, but much still remains to be learnt. In particular, the phenomenon of modification by which the eutectic microstructure is converted from a coarse flake to a fine fibrous morphology by trace additions of sodium or other modifying agents remains unexplained, and is likely to remain so until a detailed study of the crystallography of the modified eutectic silicon is achieved.

The flake–fibre transition is known [1, 2] to occur without modifying additions when an Al–Si alloy is undercooled to some critical degree below the equilibrium eutectic temperature. It has also been observed [3] that the frequency of twinning in the silicon phase increases with undercooling, which led to the proposal that the greatly increased flexibility of growth habit in the modified eutectic is made possible by a very high frequency of multiple twinning in the silicon phase, which permits repeated branching of the silicon phase to maintain a stable solid–liquid interface. However, experimental data on the crystallography of the modified silicon is so limited it is possible to suggest [4, 5] that twins are not present in the modified structure.

There are other unsolved questions that relate to the flake–fibre transition. It seems that silicon has an intrinisic tendency to form twins during nucleation and growth from an Al–Si melt and the reason for this has not been established. In a modified alloy the eutectic arrest occurs at substantial undercooling, ΔT, in the range 5 to 10°C [6] compared with maximum $\Delta T < 1°C$ for normal (lamellar or fibrous) eutectic structures [7]. The difference has been attributed [8] to a large diffusion distance between phases at the growth interface, imposed by the anisotropic growth of the silicon. Flood and Hunt [5] have shown that the relationship between interphase spacing, λ, ΔT and solid–liquid interface velocity (v) are consistent for the modified eutectic structures, so that it can be assumed that the factor inhibiting reduction of diffusion distance is the same for both morphologies. This appears to be related to the limited ability of the eutectic silicon to branch or bend through random angles. A third question relates to the observation that the silicon phase leads the aluminium phase by a large margin at the growth interface of the unmodified eutectic [3, 9] but that this lead disappears in the modified structure, with a possible tendency for the aluminium to overgrow the silicon [6]. This change occurs as freezing rate is increased, as well as on the addition of modifying agents, and has been associated with the degree of undercooling of the melt.

Answers to these questions are unlikely to be found without more detailed information on the crystallography of the modified eutectic, but some

*Present address: Department of Metal Science and Technology, Kyoto University, Sakyo-ku, Kyoto 606, Japan.

0022–2461/85 $03.00 + .12 © 1985 Chapman and Hall Ltd.

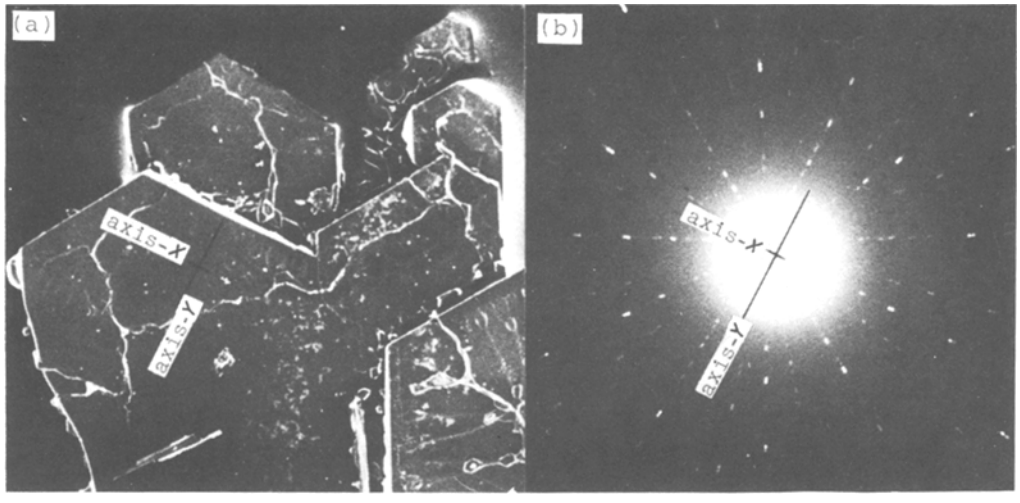

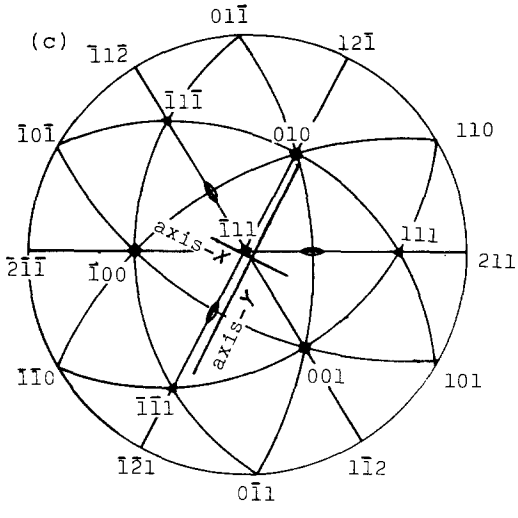

Figure 1 (a) Scanning electron micrograph of extracted plate-like primary silicon in Al–16 wt % Si alloy. (b) X-ray diffraction Laue pattern of spot indicated by cross in (a). (c) Stereographic projection with the X-ray incident beam direction as the projection pole.

light is thrown by more recent crystallographic studies of coarser microstructures containing primary silicon and flake-type eutectic silicon.

2. Primary silicon and the effect of sodium

The form of primary silicon crystals in Al–Si alloys varies with composition and formation temperature [10]. Equi-axed faceted crystals are observed [4] but the most familiar form is plate-like, as in Figs. 1–4. The plates may be simple hexagons, as shown diagramatically in Fig. 5, or several plates may radiate from a centre of nucleation, as in Fig. 4 where the plate surfaces lie normal to the plane of the paper. In either case the plate surfaces lie parallel to {1 1 1}, which is also the twinning plane, and there is general agreement [6, 11] that edgewise growth in the ⟨2 1 1⟩ directions occurs by the twin plane re-entrant edge (TPRE) mechanism originally proposed for the plate-like growth of germanium crystals [1, 2, 13, 14]. Crystal growth in the diamond cubic system is anisotropic, with the slowest growth direction normal to the closest packed {1 1 1} planes, so that there is a strong tendency for the less close-packed planes to grow out, until the crystal is faced only by

Figure 2 Scanning electron micrograph of extracted plate-like primary silicon in Al–16 wt % Si alloy. Multiple twin plane re-entrant angles revealed at plate edge.

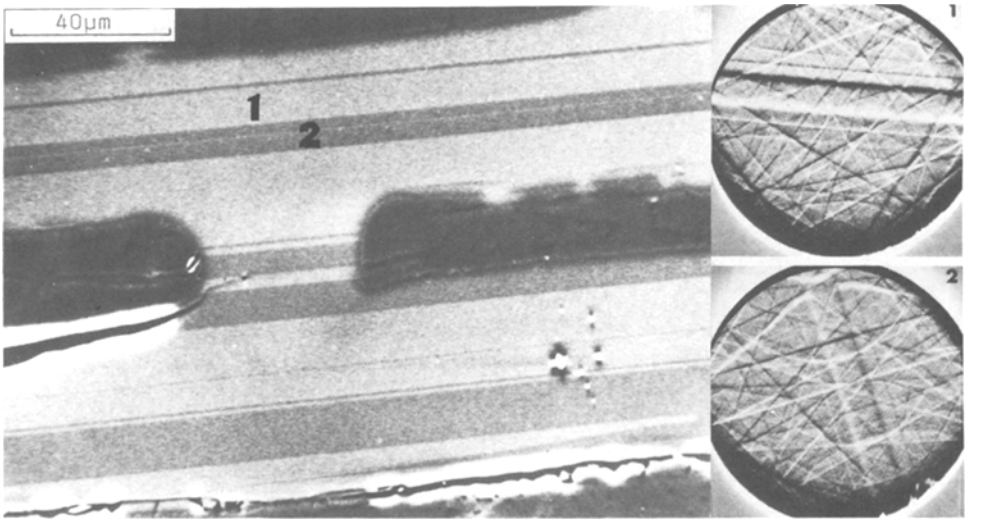

Figure 3 Plate-like primary silicon crystal showing multiple twinning. Back-scattered electron scanning image of a polished surface. Selected area electron channelling patterns at points 1 and 2 show twin relationship.

{1 1 1} facets [15]. If the crystal contains two or more twin planes (Fig. 3) however, self-perpetuating grooves faced with {1 1 1} planes can form where the twin planes terminate at the surface, with included angle 141°, as shown in Fig. 5. The grooves act as preferential sites for attachment of silicon atoms from the melt, permitting a growth rate in ⟨2 1 1⟩ directions much higher than ⟨1 1 1⟩ growth. Measurements by Steen and Hellawell [8] indicate a growth rate advantage of about 5 : 1. Grooves at a growing edge are shown in Fig. 2. Fig. 1 shows the active ⟨2 1 1⟩ growth directions in a plate crystal trending to the hexagonal shape. The {1 1 1} surfaces of the plates are by no means inactive and ⟨1 1 1⟩ growth tends to develop from isolated points on the surface, sometimes giving rise to a second parallel plate as in Fig. 3. This corresponds to the antiskeletal growth mode defined by Chernov [16, 17].

When a hyper-eutectic Al–Si alloy is over-modified by sodium, the growth mode of the primary silcion crystals tends to change to a roughly spheroidal form [4, 6], as in Fig. 6. The spheroid surfaces are faceted as in Fig. 7, and as reported by Fredriksson *et al.* [4]. The spheroid in Fig. 6 was sectioned through its centre and the back-scattered electron scanning image of Fig. 6b shows light-coloured bands radiating from centre

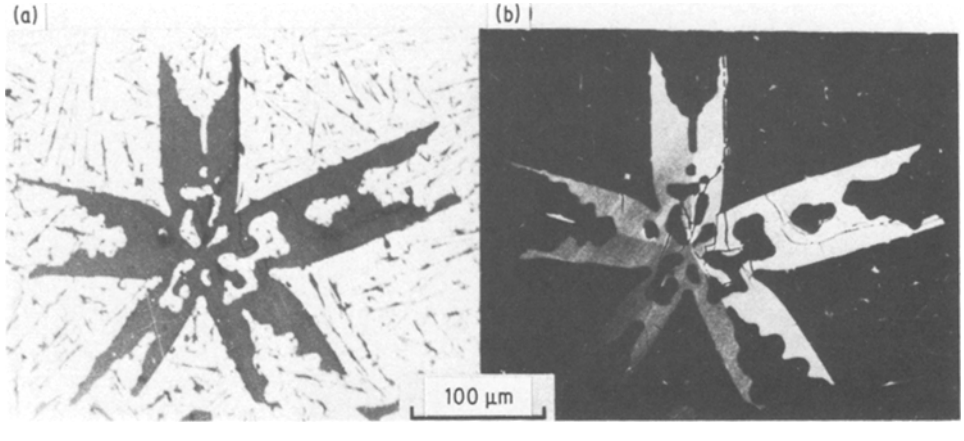

Figure 4 Primary silicon in an unmodified Al–Si alloy. (a) Optical micrograph showing five silicon platelets with a common point of nucleation. (b) Back-scattered electron scanning image showing contrast across twin boundaries. Electron channelling patterns showed that each branch is twinned.

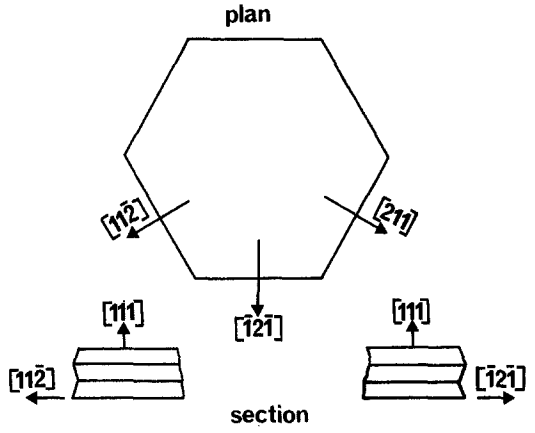

Figure 5 Multiple twinning in diamond cubic crystal showing alternate re-entrant edges and grooves [6].

to periphery of the crystal [11]. Similar bands have been observed using a suitable etchant [18]. Electron microprobe line scans and X-ray images showed that the sodium in the crystal was concentrated in these bands. Radial cracks were closely associated with the bands. Similar sodium-rich bands and crack distribution were regularly observed in other silicon spheroids [11].

The crystallography of the spheriods was investigated by identifying the surface facets of extracted primary crystals (Fig. 7) using Laue X-ray diffraction and by electron channelling patterns (ECP) on sections through spheroids (Fig. 8). The surface facets were found to be most frequently parallel to {111} but some facets were parallel to less densely packed planes such as {100} and {211}. The combination of facets was such that the spheroids could not be monocrystalline and the ECP patterns on cross-sections identified a limited number of twin-related grains. In Fig. 8 the boundaries revealed in the back-scattered image separate two grains, E and F, in twin relationship, but in other spheroids much more complex twin relationships existed.

From these relationships it was concluded [11] that a spheroidal silicon crystal is composed of several pyramidal grains with their apices at the centre of the sphere. The sodium-rich regions are found at the boundaries of these grains and many or all of the grains are twin-related. One effect of this growth pattern is that the surface of a spheroid is largely composed of low energy {111} planes, though less completely so than the plate-like crystals of Figs. 1 and 2. This suggests that the sodium-modified primary crystals are constrained to grow in a mode which minimizes solid–liquid surface energy. This might be expected if interface velocity is controlled by diffusion in the melt.

Any explanation for this growth pattern must account for the presence of twins, the suppression of the TPRE growth mechanism and the predominance of {111} facets. A mechanism of nucleation and growth can be proposed related to that postulated in [19] for the formation of five-fold twinned silicon crystals such as that in Fig. 4. It is believed that this branched crystal nucleates by aggregation of silicon tetrahedra pre-existent in the melt, the initial nucleus being an aggregate of five tetrahedra forming a decahedron. Near the critical nucleus size, when surface-to-volume ratio is very large, this configuration has an energy advantage, because the tetrahedral faces become low energy {111} crystallographic planes. Growth starts as a roughly equi-axed crystallite in which the surfaces in contact with the melt are {111}, giving a lower surface energy than an idiomorphic single crystal with higher energy faces exposed

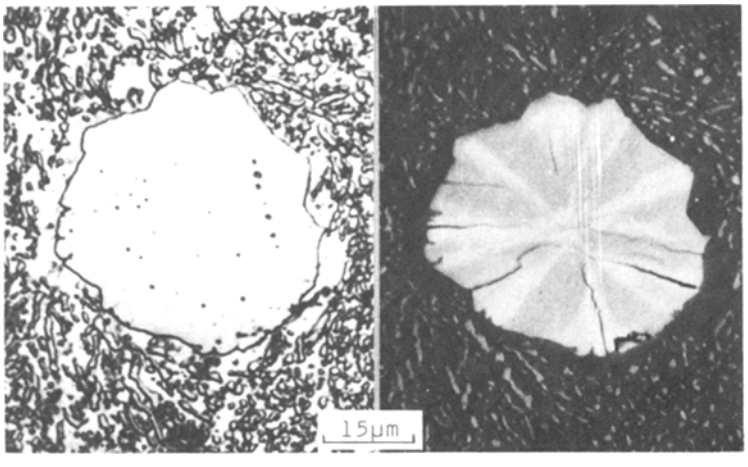

Figure 6 Spheroidal primary silicon in sodium-treated Al–16 wt % Si alloy. (a) Photomicrograph. (b) Back-scattered electron scanning image. Plane of polish passes through centre of spheroid. Light steaks are sodium-rich. Note radiating cracks.

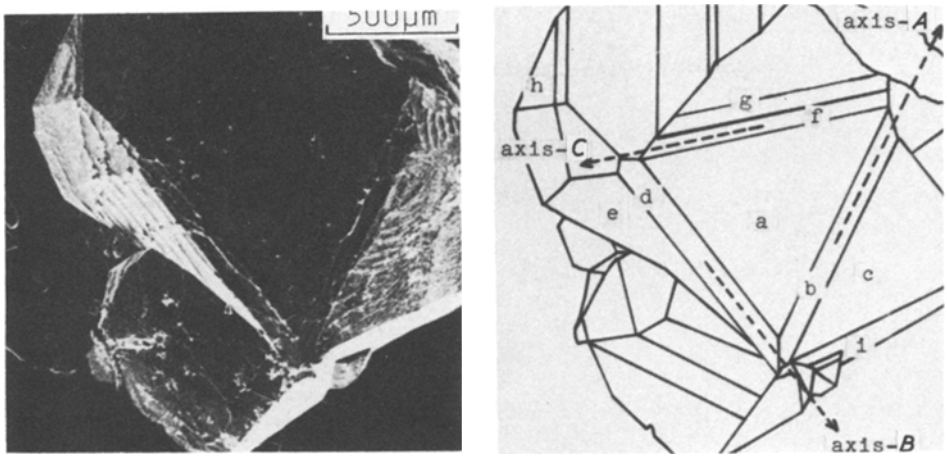

Figure 7 Scanning electron micrograph of extracted primary silicon spherulite in Al–16 wt % Si with large additions of sodium, and its schematic figure, illustrating the crystal facets used for X-ray diffraction analyses.

[20]. However, as the particle grows and surface-to-volume ratio decreases the energy advantage diminishes. There is also a strain energy term, because five tetrahedra do not fit exactly to form a decahedron and must be slightly distorted to overcome this misfit. As the particle size increases this strain increases and causes instability. For the five-branched particles of Fig. 4 the instability results in a change of growth mechanism, for which an explanation has been proposed [19]. The effect is that each twinned branch continues to grow as a flat plate by the TPRE mechanism.

For the sodium-modified spheroidal crystals a similar mode of nucleation is proposed, since an aggregate of silicon tetrahedra would automatically initiate the observed twin planes. However, the number of twins in the grown crystals varies widely and this could be attributed to a variable number and arrangement of tetrahedra in the original nuclei. During later growth the primary particles retain an equi-axed shape as they grow to large size and the TPRE growth mechanism is suppressed. The observation that sodium is concentrated at twin boundaries strongly supports the concept [3, 21] that the sodium addition acts to

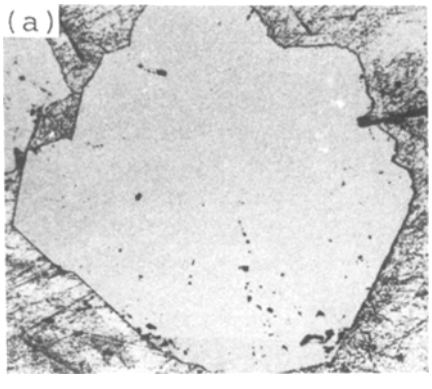

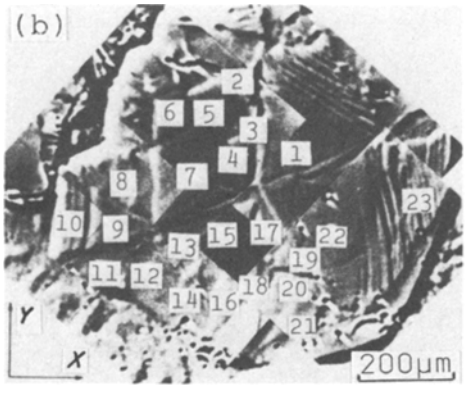

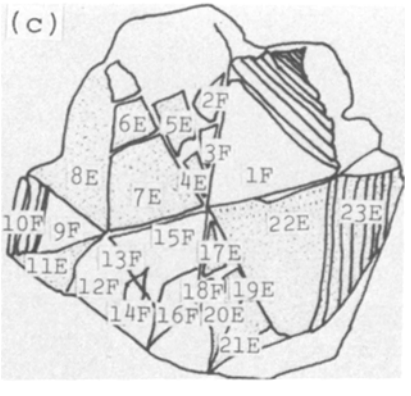

Figure 8 Section through primary silicon spheroid in sodium-treated Al–16 wt % Si alloy. (a) Photomicrograph. (b) Back-scattered electron scanning image. Numbers indicate positions analysed with ECP. (c) Regions of two different crystal orientations (E and F) revealed by ECP. E and F are twin-related.

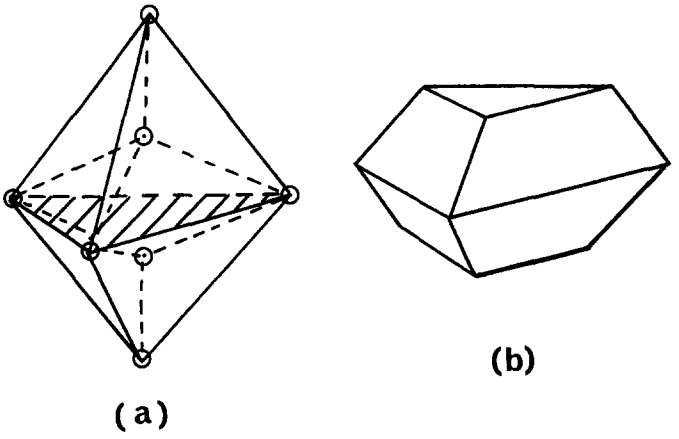

Figure 9 (a) Silicon tetrahedra with {1 1 1} mirror plane (shaded). (b) Truncated tetrahedra at later stage growth.

poison the re-entrant grooves that might tend to form in the early stages of growth and would lead to plate-like growth forms as in Figs. 1 and 4. The poisoning could be by preferential attachment of sodium to the groove surfaces but, whatever the mechanism, the effect must be to reduce the rate of attachment of silicon atoms to the groove surfaces so that the growth rate advantage of the TPRE mechanism is lost or minimized.

When TPRE growth is suppressed, the crystal will be forced into isotropic growth, but the tendency to minimize solid–liquid interfacial energy during growth will remain and is observed to result in a spheroidal shape, with the major part of the surface being composed of low energy {1 1 1} planes. This configuration can only be achieved in the presence of growth twins and the development of twins is adequately accounted for if nucleation occurs by the aggregation of silicon tetrahedra. Ino [20] discusses the critical energies for nucleation of a variety of particle shapes formed in this way, of which one favourable form is an icosahedron, an equi-axed form from which the particle in Fig. 7 could well have developed. However, as mentioned above, it is unlikely that the nucleus has any fixed morphology.

The concept of nucleation by aggregation of tetrahedra is strongly supported by the invariable appearance of cracks radiating from the centre of growth, as in Fig. 6. Any assembly of tetrahedra to form a solid body will be associated with elastic strain energy, because tetrahedra do not fit exactly to form an equi-axed shape [19, 20]. The strain energy increases as the particle grows and must eventually be relieved. The major relief apparently occurs by cracking, but sodium in solution expands the silicon lattice so that the concentration of sodium at the radiating twin boundaries must play a part in reducing the elastic strain energy and thus stabilizing the spheroidal shape. It may also be true that sodium reduces the twin boundary energy and thereby facilitates twin formation.

3. Nucleation of flat-plate silicon

The evidence above suggests that multiple twin formation in silicon crystals, as in Figs. 4 and 8, results from chance aggregation of silicon tetrahedra pre-existing in the melt as discussed in detail in [9]. The subsequent crystal form depends on the number of tetrahedra participating, e.g. primary silicon crystals with K and L shapes are also regularly observed. There must, then be a form of nucleus which would give rise to the frequently observed flat plate form, as in Fig. 2, with twins parallel to the surface as in Fig. 3. An appropriate form of embryo is an assembly of two tetrahedra as in Fig. 9a. If this grows to critical nucleus size by attachment of single silicon atoms to the surfaces the faces can develop into favourable low energy {1 1 1} facets while the central mirror plane becomes a {1 1 1} twin plane. If many embryos such as Fig. 9a exist in the melt near the liquidus temperature, it can be expected that some will attach to nucleant particles in the melt (such as phosphide particles) or to mould walls and grow to critical size. The double tetrahedron shape is not ideal for minimizing surface area and the surface-to-volume ratio can be further reduced as the nucleus grows if the two apices are truncated to produce a more nearly spheroidal shape as in Fig. 9b. {1 1 1} planes parallel to the central twin plane would form readily, preserving the advantage of low energy facets. These new surfaces form suitable points of attachment for additional silicon tetrahedra from the melt, forming twin planes parallel to the first. If two or more twin planes

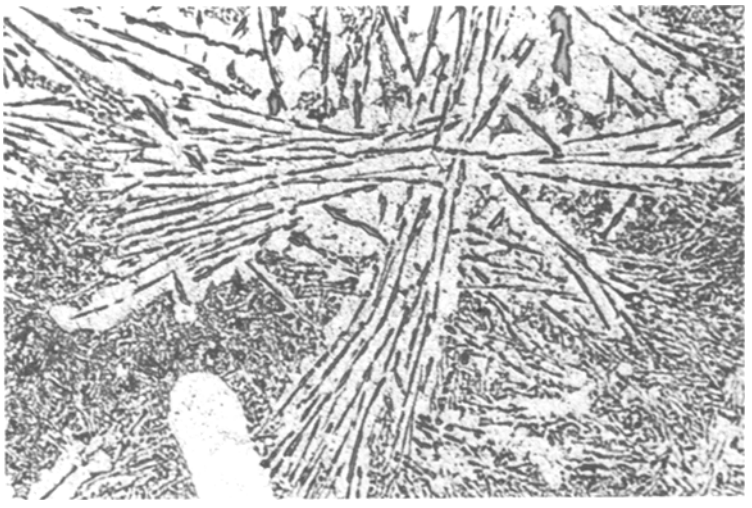

Figure 10 Al–12 wt% Si cooled in furnace and quenched after half solidification. Flake silicon eutectic nodule and wheatsheaf configuration. × 240.

form in this way the condition is established for formation of a twin plane re-entrant edge, as in Figs. 2 and 5. Growth in a ⟨2 1 1⟩ direction at this edge will be much faster than growth normal to the {1 1 1} planes, so that the crystal will expand into a flat plate with relatively inert {1 1 1} faces. It is probable that the ratio of tetrahedra to single Si atoms increases as melt temperature falls, especially as the melt is undercooled below its liquidus. This could account for the absence of twins in eutectic silicon grown at very slow rates, less than about 4 μm sec^{-1} [3], and the increase in twin frequency with increasing undercooling as growth velocity increases.

An alternative nucleation sequence can be suggested on the basis of Bernal's studies of "random close-packing" of atoms in liquids. Bernal [22] observed the frequent occurrence of "collineations", or groups of as many as eight atoms arranged in a straight line. In Fig. 9a the two centred atoms and the apices lie in a straight line. If these are pre-existent, the addition of three atoms to form the mirror plane could then occur very readily, with tight bonding at the natural angle of 109.5°. A longer collineation would permit the formation of additional closely-spaced parallel twin planes.

4. Plate-like eutectic silicon

In unmodified alloys, for growth conditions defined as Region C by Day and Hellawell [3] the silicon phase in the eutectic grows as thin flat plates with a growth mode very similar to that of the flat plate primary silicon. The plates tend to form radiating clusters as in Fig. 10, sometimes referred to as a "Wheatsheaf" configuration. A given plate usually grows straight for some distance, then may branch or change direction through a large angle, in response to local conditions at the growth interface. X-ray diffraction photos indicate a random crystal orientation of both the silicon and aluminium eutectic phases [3, 9], but the possibility of an epitaxial relationship between the phases on a much finer scale was investigated [23] by electron diffraction of thin films. The samples were prepared by dipping a loop of iron wire into a melt and withdrawing slowly, so that a thin flim of solid alloy formed across the loop. The microstructures obtained in this way appeared to be identical with those obtained by sectioning of bulk specimens. Orientation relationships observed between the eutectic phase fell into three groups, of which the most frequent was:

$$[0\,0\,1]\ \mathrm{Al}\,//\,[1\,1\,0]\ \mathrm{Si};\quad [1\,0\,0]_{\mathrm{Al}}\,//\,[\bar{1}\,1\,\bar{1}]_{\mathrm{Si}}$$

Analysis of the diffraction patterns and dark field images from the same samples confirmed that growth occurs by the TPRE mechanism and demonstrated that branching and direction changes of the silicon plates or flakes occur by multiple twinning.

Fig. 11a shows schematically the growing tip of a eutectic silicon flake, consisting of alternate twin crystals labelled Si(A) and Si(B). The plate surfaces are {1 1 1} and, if {1 1 1} planes are exposed at the growing tip, they would necessarily form the 141° re-entrant angle shown, which is the condition for TPRE growth in the ⟨1 2 1⟩ direction [6, 13, 14]. The plates tend to thicken in places by

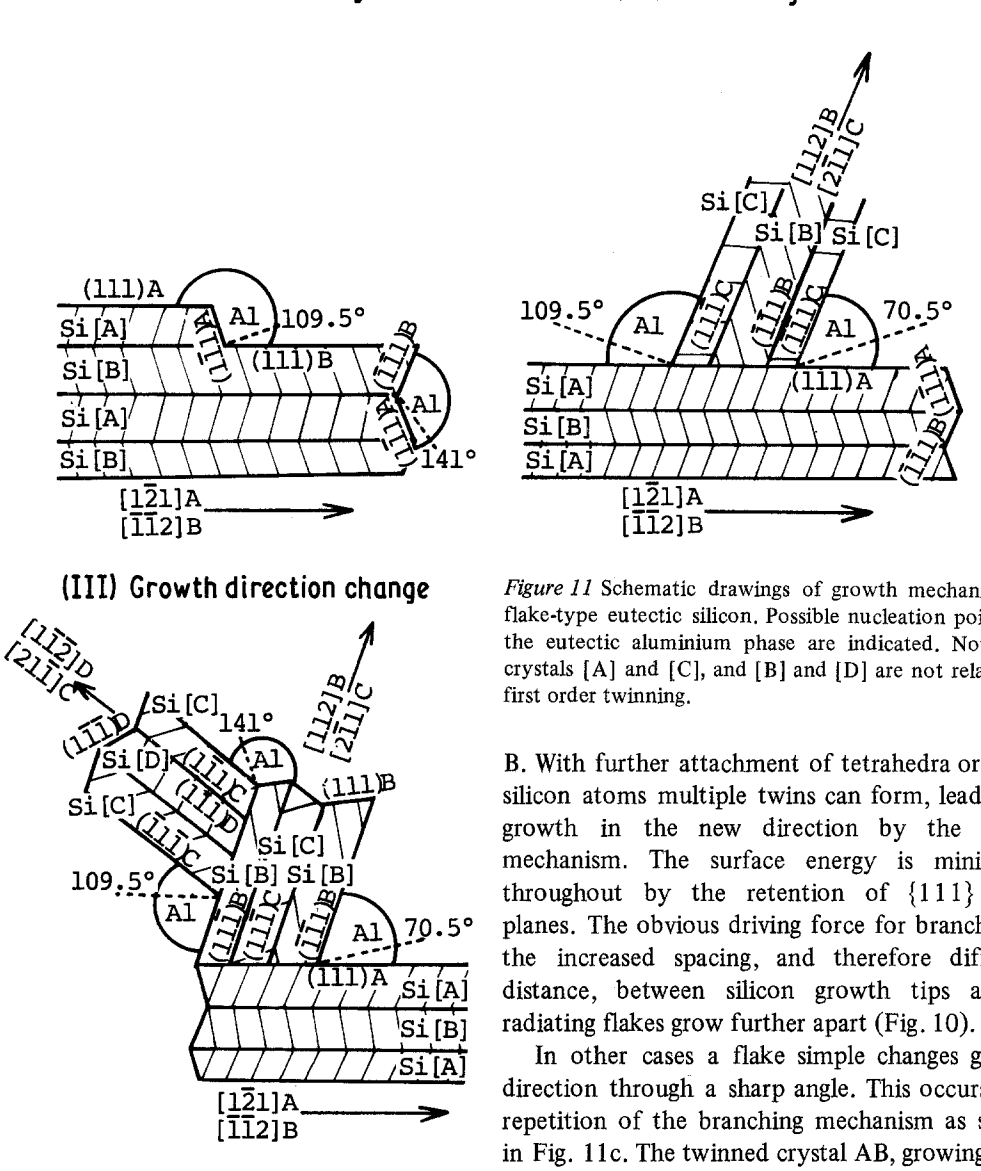

Figure 11 Schematic drawings of growth mechanisms in flake-type eutectic silicon. Possible nucleation points for the eutectic aluminium phase are indicated. Note that crystals [A] and [C], and [B] and [D] are not related by first order twinning.

addition of a further twinned layer, which would form the 109.5° growth step shown.

Branching was observed as in Fig. 11b. The original crystal with alternate twins A and B branches by twinning at a {1 1 1} plane to give a 70.5° direction change. The branch contains two crystals B and C in twin relationship. Crystals A and C are not twin-related. It can be assumed that the branching commenced by nucleation of a twinned crystal B on A and subsequent formation of the crystal C in twin relationship with B. Alternatively, a twinned double tetrahedron as in Fig. 9a could attach itself to the {1 1 1} surface so that one half (B) is in twin relationship with A and the other half is already in twin relationship with B. With further attachment of tetrahedra or single silicon atoms multiple twins can form, leading to growth in the new direction by the TPRE mechanism. The surface energy is minimized throughout by the retention of {1 1 1} habit planes. The obvious driving force for branching is the increased spacing, and therefore diffusion distance, between silicon growth tips as the radiating flakes grow further apart (Fig. 10).

In other cases a flake simple changes growth direction through a sharp angle. This occurs by a repetition of the branching mechanism as shown in Fig. 11c. The twinned crystal AB, growing from right to left, gives rise to the twinned crystal BC, with a change of growth direction of 109.5°. The crystal BC gives rise in turn to the crystal CD at an angle of 70.5°. The net change in growth direction from the original crystal is 39°. Combinations of this type allow the growing silicon flake to change direction through almost any angle while retaining the ⟨1 1 2⟩ growth direction and the {1 1 1} surface planes. This rapid sequence of changes in response to local variations in growth conditions requires a very simple method of nucleating the twinned branches. The attachment to {1 1 1} surfaces of silicon tetrahedra pre-existing in the melt would automatically produce the required twin configurations and is therefore a satisfying postulate.

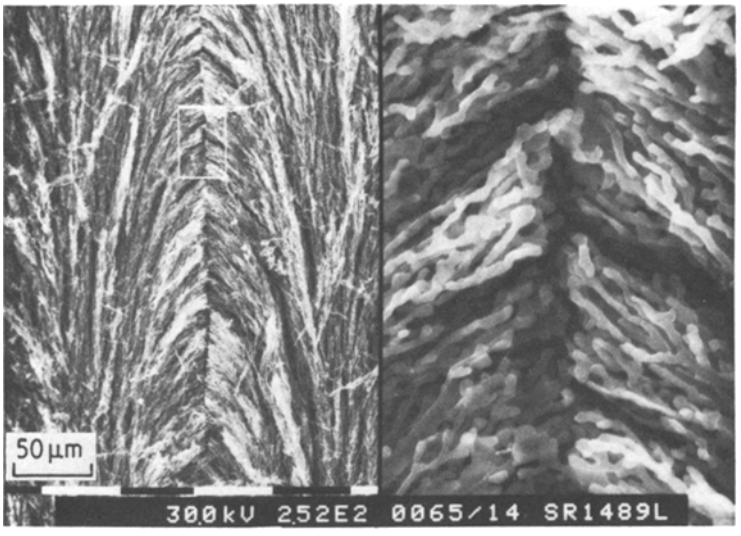

Figure 12 Al–14% Si–0.18% Sr. longitudinal section, growth direction bottom to top. $v = 89\,\mu m\,sec^{-1}$. (a) modified eutectic silicon, × 242. (b) enlargement of marked area in (a), × 1760. Aluminium phase removed by etching to reveal eutectic silicon.

5. The flake–fibre transition

The most notable effect of modification is a dramatic change in the morphology of the eutectic from the flake or plate-like form described above to a highly branched fibrous form sometimes likened to seaweed. Modification can be accomplished by the addition of as little as 0.01 wt% Na, by a high freezing rate or by other modifying elements, including Sr. There are no readily detectable differences in the modified eutectic structure whether modification is by sodium or strontium (impurity modification) or by fast cooling (chill modification). Chill modification requires a much higher solid–liquid interface velocity [1] and it may be less effective in improving mechanical properties than impurity modification [6]. The sodium-modified eutectic silicon shown in Fig. 12 has branched, rounded fibrous with very little obvious relationship to the flake form in unmodified eutectic (Fig. 10). The growth direction of the silicon fibres has been observed as ⟨1 0 0⟩ [2, 24] or ⟨1 1 0⟩ [1] but ⟨1 2 1⟩ occurs rarely [1] so that growth is unlikely to be by the TPRE mechanism. Multiple twinning on {1 1 1} planes in the silicon has been observed [1, 2] but there has not, as yet, been any detailed electron diffraction study of the type described above for the unmodified eutectic. None the less, it is possible to make some inferences about the effects of sodium in modification on the basis of the observed effects in coarser structures, together with a clarification of the related undercooling phenomenon which was achieved by Flood and Hunt [5].

Attempts to explain the mechanism of the flake–fibre transition have been complicated by the long-standing observation that refinement by sodium addition is accompanied by a large increase in undercooling of the eutectic arrest. Any mechanism proposed to account for the structural change has also to account for the undercooling increase. However, observations by Flood and Hunt [5] show that the increased undercooling is a separate phenomenon which is associated with the structural change but is not directly caused by the sodium addition. The large undercooling change is observed when a flake structure formed by endogenous freezing is compared with a fibrous structure formed by exogenous freezing. The two are not comparable, even though the casting conditions may be identical.

In endogenous freezing the solid–liquid interface forms as a wave of eutectic nodules continuously re-nucleated in the melt ahead of the fully solid interface [5, 10]. In exogenous freezing nucleation occurs only at the chill surface of an ingot and solidication progresses by growth of columnar eutectic grains until they meet at the ingot centre. In sand-casting of an unmodified Al–Si alloy the normal freezing mode is endogenous whereas the modified fibrous structure formed under identical casting conditions has no such tendency. Freezing is always exogenous. In the present context the essential difference is that the solid–liquid interfacial area of the growing unmodified eutectic is the sum of the surface areas of all the separate nodules plus that of the following fully solidified interface. The total

interfacial area is therefore many times larger than that of the smooth interface formed by the modified fibrous structure in a casting of similar dimensions. In the case calculated by Flood and Hunt the ratio was 18 : 1. The eutectic arrest temperature is determined by a balance between the rate of heat extraction from the casting and the rate of heat production at the solid–liquid interface. The rate of total latent heat production is proportional to the interfacial area and, if local interface velocities were equal, this rate would be 18 times as high for the unmodified as for the modified casting.

However, if the rate of heat extraction from the two castings is equal it must be balanced by an equal rate of latent heat production. To achieve this the interface velocity of the unmodified eutectic must be slower than that of the modified eutectic by a ratio equivalent to the area ratio. It was shown by Flood and Hunt that, when this is taken into account, the flake and fibrous eutectic structures both conform with two equations used to describe normal eutectic freezing:

$$v = A\,\Delta T^2 \qquad (1)$$

$$\Delta T = Bv\lambda + C/\lambda \qquad (2)$$

where v is the eutectic liquid interface velocity, λ is the interflake or interfibre spacing, $\Delta T = T_e - T$ where T is the interface temperature during growth, T_e is the equilibrium eutectic temperature. A, B and C are constants.

If A, B and C are assumed to be the same for both structures, and endogenous growth is taken into account the equations predict the type of variation in ΔT and λ which is observed. For constant A, Equation 1 requires that the higher interface velocity of the modified eutectic is balanced by a higher undercooling than for endogenous growth of the unmodified eutectic. Established observations [6] indicated that modification of a casting increases ΔT by a factor of 7 or more and Flood and Hunt [5] observed a similar ratio.

The undercooling difference also requires a difference in λ spacing. In Equation 2 the C/λ term is related to interfacial energies and has been shown [25] to make only a minor contribution to undercooling, so that to a first approximation $\Delta T = Bv\lambda$. Measurements of Hillert and Lange [4] indicate that both flake and fibre structures conform to the relationship $\lambda^2 v = D$, where the constant D is of similar magnitude for both morphologies. Substituting in $\Delta T = Bv\lambda$ we obtain $\Delta T = BD/\lambda$ and $\Delta T_m/\Delta T_{um} = \lambda_{um}/\lambda_m$ where m and um denote modifed and unmodified. It follows that the relatively large undercooling of the modified structure demands a relatively large λ spacing for the unmodifed flake structure if B and D are roughly the same for flake and fibrous growth.

A corollary to these results is that, if the flake and fibre structures are grown at the same interface velocities, they should have similar λ spacings. Comparison is possible because the flake structure can be constrained to grow exogenously by the application of a high positive temperature gradient, as in unidirectional freezing experiments, while the sodium-modified eutectic can be grown at low interface velocities. Graphs of log λ against log v prepared by Fredriksson *et al.* [4] for the flake and fibrous morphologies are almost identical for growth rates between 1 and 1000 mm h^{-1} (0.3 to 277 μm sec^{-1}), suggesting that the constants A and B are identical for both morphologies. More recent measurements show differences which appear to be significant.

Flood and Hunt [5] found $A = 0.43 \times 10^{-6}$ m sec^{-1} K^{-2} for the sodium-modified fibrous structure and $A = 0.37 \times 10^{-6}$ for the flake structure. Substitution in Equation 1 indicates a 7% difference in ΔT for the same interface velocity but this is negligible by comparison with a difference of the order 700% due to endogenous freezing of the flake eutectic.

Glenister and Elliott [26] measured undercoolings in directionally solidified strontium-modified fibrous eutectic, from which a value of $A = 0.33 \times 10^{-6}$ m^2 sec^{-1} K^{-2} is obtainable, in reasonable agreement with Flood and Hunt's value for the sodium-modified structure. The same authors [27] measured interface undercoolings during directional solidification of the flake silicon eutectic. For a low applied temperature gradient and $v = 100\,\mu$m sec^{-1} their figures give a value of $A = 1.56 \times 10^{-6}$ m sec^{-1} K^{-2}. On this basis the interface undercooling of the fibrous eutectic would be about twice that for the flake silicon at the same interface velocity, e.g. at $v = 100\,\mu$m sec^{-1}, $\Delta T \simeq 8°$C for flake silicon and $\Delta T \simeq 16°$C for fibrous silicon [28]. This ratio is affected by both applied temperature gradient, G, and interface velocity, v, but is generally much smaller than the ratios observed by measurements of arrest temperatures in sand castings.

It is apparent that the major part of the increased undercooling assoicated with modification can be attributed to the change from endogenous to exogenous growth. There remains a relatively small difference, the cause of which has yet to be determined. Variations in interfacial energies or relative diffusion rates are possible factors.

Although both structure types conform with Equation 2, the measured λ spacings are much larger than those observed in non-faceted eutectics at similar growth velocities, e.g. at $v = 15\,\mu m\,sec^{-1}$ the λ spacing $\simeq 1.5\,\mu m$ in the normal eutectics of Pb–Sn and Al–$CuAl_2$ [29] whereas at the same velocity the average λ in flake silicon eutectic ranges from 8.5 to 11.4 μm, dependent on gradient ([28] p. 163) while for impurity modified eutectic $\lambda \simeq 3.7\,\mu m$. Hellawell and co-workers [8, 25] attribute this, for the flake-type eutectic, to the rigidity of the eutectic silicon plates, which prevents the rapid adjustment of the growth front necessary to maintain the minimum λ required for efficient interphase diffusion.

This large diffusion distance also implies a large undercooling of the eutectic arrest by comparison with normal eutectic growth. If $\Delta T = Bv\lambda$, a large λ implies a large ΔT for given v. At $v = 15\,\mu m\,sec^{-1}$ Toloui and Hellawell [25] measured undercoolings varying from 2.7 to 14.3 K, increasing with decreasing applied gradient. For the lamellar Pb–Sn eutectic Jordan and Hunt [30] measured $\Delta T \simeq 0.5$ K for similar velocity. A large kinetic undercooling of the silicon may contribute to this difference but has been shown to be insufficient to be the prime cause [8].

The observation that Equation 2 applies equally to the flake and fibrous morphologies suggests that the factors maintaining a large diffusion distance at the interface operate in much the same way for both morphologies, although less restrictively for the more flexible fibrous structure. It would follow that the elaborate branching mechanisms described above (Fig. 11) continue to operate on a finer scale in the fibrous silicon. This would require the high twin frequency at large undercoolings predicted by Day and Hellawell [3]. A high density of twin traces has been observed in fibrous silicon [1, 2, 31] but their relationship to the growth mechanism is yet to be determined.

6. Structural differences

The significant differences between the unmodified flake and modified fibre microstructures appear to be:

(a) In the unmodified eutectic the silicon flakes lead the aluminium phase at the eutectic–liquid interface by a distance $S_\beta > \lambda$. In the modified eutectic $S_\beta \simeq 0$ [8, 25].

(b) The aluminium phase is polycrystalline within a single eutectic grain in the unmodified eutectic [2, 3, 23, 31] but monocrystalline in the modified eutectic [2].

(c) In the unmodified eutectic the silicon flakes grow consistency in ⟨1 2 1⟩ directions [6, 23]. In the modified eutectic the fibre growth direction is probably ⟨1 1 0⟩ or ⟨1 0 0⟩ but ⟨1 2 1⟩ is unusual [1, 2, 24]. Together with the rounded shape of the fibres this indicates that the TPRE growth mechanism does not operate in fibrous growth.

A definition of "eutectic grains" is required in this context. In the modified eutectic a grain has a single point of nucleation at a chill surface and will normally grow in columnar fashion until terminated. The aluminium phase is monocrystalline within one columnar grain but if the silicon phase is frequently twinned it should appear polycrystalline in X-ray diffraction. This does not seem to have been tested experimentally but a preliminary exploration by transmission electron microscopy [31] shows branching occurring by a twinning mechanism in eutectic fibres.

The unmodified eutectic grows in the "wheatsheaf" morphology of Fig. 10. The photograph shows endogenous growth, in which several sheaves grow from a point of nucleation in the melt to form a rounded eutectic nodule which later joins with neighbours to form a continuous, but irregular, solidification front. In ingots or castings this would occur with a near-zero temperature gradient in the melt and constitutional undercooling due to impurity elements should be high, permitting easy nucleation in the melt on suitable nucleant particles such as AlP.

In laboratory-scale unidirectional growth experiments, the materials used are usually of high purity and a steep temperature gradient is applied to make the solid–liquid interface as flat as possible. Hence constitutional undercooling is severely reduced and nucleation in the melt becomes difficult. A relatively flat, though ragged, solid–liquid interface is formed and this corresponds to exogenous growth, although some nucleation in the melt occurs at low gradients [25]. However the wheatsheaf growth mode

still operates. Each sheaf can grow for a limited distance before it becomes unstable and eutectic growth is continued by initiation of a new sheaf. Under a steep temperature gradient the new sheaf tends to initiate by growth from a silicon flake at the periphery of a prior unstable sheaf, so that the silicon phase is essentially continuous. For present purposes each sheaf is regarded as a eutectic grain.

The instability of a sheaf can be attributed to the lead distance S_β. It has been shown [9] that, if $S_\beta \simeq \lambda$, interphase diffusion is unable to maintain a common Al–Si growth front. The aluminium phase is forced to re-nucleate repeatedly between the silicon plates in order to maintain an approximately equal linear growth rate of the two eutectic phases. It follows that the aluminium phase is polycrystalline, with a grain size substantially smaller than the size of a single eutectic grain, or individual sheaf [2]. The epitaxial relationship [23] mentioned above suggests that the aluminium grains nucleate on the side faces of the silicon flakes, encouraged by accumulation in the liquid of aluminium rejected by the growing silicon. The lead distance S_β must then be highly variable and it is to be expected that such a fluctuating growth process would lead to instability. It is surprising that the process can conform so closely to Equations 1 and 2, which were developed to account for normal lamellar and fibrous growth, but the evidence that the aluminium phase is polycrystalline at the time of formation [2, 9] is supported by electron diffraction studies [23, 31] and cannot be disregarded. None the less it seems obvious that diffusion coupling must be more efficient in the growth of the fibrous structure, so that a real difference between the constants in Equations 1 and 2 probably exists for flake and fibrous growth.

7. The mechanism

Since the anomalous undercooling behaviour in sodium modification has been explained as a secondary effect, it remains for a model of the modification mechanism to account for the change from polycrystalline to monocrystalline aluminium and the apparent disappearance of the TPRE mechanism. The remaining structural change is the removal of the lead distance S_β and it is not unreasonable to suggest that this is the operating factor which trips the flake–fibre transition. The reduction of S_β to zero removes the reason for the re-nucleation of the aluminium phase during growth. The disappearance of the TPRE mechanism may be a separate effect which occurs simultaneously. For both effects different causes can be looked for in chill modification and impurity modification.

8. Chill modification

An essential characteristic of eutectic growth conforming to Equations 1 and 2 is that the two phases must advance at the same velocity at a common growth front. However they can be considered as having different potential growth rates in the eutectic melt and the phase with the faster potential rate should lead the other at the growth front. On this basis Tiller [32] proposed that a large lead distance would be favoured by a large difference in liquidus slopes and distribution coefficients for the two phases. Davies [18] developed an expression to predict the lead distance from phase diagram data:

$$S_\beta = -\tfrac{1}{2}\lambda_\beta\left(\frac{m_\alpha}{m_\beta}\frac{V_\alpha}{V_\beta}+1\right) \qquad (3)$$

where m_α and m_β are the liquidus slopes, V_α and V_β are volume fractions in the eutectic, and λ_β is the thickness of β lamellae (in this case Si).

With increasing velocity λ and λ_β decrease, with a corresponding decrease in S_β, but the critical quantity is likely to be S_β/λ_β, which would be constant if the expression in brackets were constant. However, there is reason to expect that V_α/V_β should also decrease with increasing velocity. The eutectic coupled region observed by Steen and Hellawell [1] indicates that eutectic growth occurs within a narrow band lying at progressively higher silicon contents as growth velocity increases. The effective eutectic composition must lie within this band, which requires that V_α/V_β must decrease as velocity increases. m_α/m_β should be essentially constant at -0.62. Steen and Hellawell show that the flake–fibre transition occurs over a range of velocities of which $400\,\mu m\,sec^{-1}$ can be taken as representative. At this velocity the effective eutectic composition can be read as 14.5% Si, compared with 12.6% Si at zero velocity. Table I compares calculated values of S_β for $v = 10\,\mu m\,sec^{-1}$ and $v = 400\,\mu m\,sec^{-1}$. λ and λ_β were calculated from $\lambda = 5\,v^{-1/2}\,G^{-2/3}$ where G K μm^{-1} is the applied temperature gradient [25] and from $\lambda_\beta = \lambda V_\beta$. $V_\alpha/V_\beta = 6.9$ at the eutectic temperature, with α phase composition

TABLE I Comparison of S_β values

G (K m^{-1})	v (μm sec^{-1})	S_β (μm)	S_β/λ_β	S_β/λ
7×10^{-4}	10	4.16	1.64	0.21
	400	0.70	1.25	0.19
150×10^{-4}	10	1.31	1.64	1.21
	400	0.24	1.22	0.18

1.65% Si and $\beta = 100\%$ Si. At $v = 400\,\mu$m sec^{-1} the estimated $\Delta T = 6$ to 10 K so that α phase $\simeq 1.5\%$ Si and eutectic = 14.5% Si. Then $V_\alpha/V_\beta = 5.62$.

Table I predicts a severe reduction in S_β with increasing applied gradient but the ratio S_β/λ is likely to be more significant and is almost unaffected by gradient. This is consistent with the observation of Steen and Hellawell that the flake–fibre transition is not sensitive to temperature gradient. The values of S_β/λ are small compared with the observation [25] that $S_\beta > \lambda$ but the Davies formula refers to strictly parallel lamellar growth and accurate numerical prediction is not be expected. Also the formula does not include the distribution coefficient, which is very much smaller for Si than for Al and would tend to increase S_β for given λ [32]. The formula predicts a decrease in S_β/λ with increasing velocity but the decrease looks too small to be effective in eliminating the lead distance. An analysis by Haworth and Whelan [33] indicates that the diffusion coefficient is likely to decrease more rapidly with falling temperature for silicon in the melt than for aluminium and this would reduce the relative rate of atomic attachment to the silicon growth tips. It seems probable that this is the major influence in reducing the lead distance. When the diffusion distance S_β/λ has been reduced sufficiently to allow silicon rejected from the aluminium phase to reach the growing silicon tips strong interphase diffusion coupling can be established and the smooth solid–liquid interface typical of fibrous eutectic growth will follow.

Simultaneous with this change in interface profile is the change from flake to fibrous morphology, which actually occurs progressively over a rather wide range of interface velocities [1]. This change can be attributed to a transition from faceted to non-faceted growth, as proposed by Flood and Hunt [5]. Silicon is considered to have an intermediate Jackson α-factor [34] so that the change from faceted to non-faceted growth occurs over a relatively small range of undercooling. At small undercooling its growth is faceted and growing crystals will be bounded by the slowest-growing {111} planes, but as undercooling increases the anisotropy of growth rate between different crystallographic directions decreases. Other faces begin to appear and eventually growth can become completely isotropic and non-faceted. An early effect of the reduction in anistropy would be to eliminate the growth rate advantage of the TPRE mechanism. It can be suggested that the transition from weak to strong coupling occurs at a temperature at which the TPRE advantage is reduced or eliminated but at which growth is still strongly faceted. The rounded appearance of the fibres probably corresponds to that of the sodium-treated primary silicon of Fig. 6, where other facets appear in addition to {111}. The similarity in λ spacings indicates that the rigidity which enforces abnormally large values in the flake morphology must largely persist in the fibrous morphology.

9. Impurity modification

Modification by addition of sodium or strontium produces the same changes in eutectic morphology as fast cooling, but the changes occur at slow cooling rates at which the mechanisms considered above cannot apply. A model is required by which sodium addition can reduce the lead distance and eliminate the TPRE advantage when undercooling is very small.

Mechanisms proposed to account for the effect of a modifying agent include:

(a) a change in solid–liquid or solid–solid interfacial energies due to accumulation of sodium at the boundaries,

(b) a reduction in diffusion rate in the liquid due to the modifier, which has differential effects on the two phases,

(c) a "poisoning" effect on the silicon plate growth mechanism which reduces its potential growth rate relative to that of aluminium,

(d) a major reduction in the transition temperature at which the silicon growth mechanism changes from faceted to non-faceted [5].

Dihedral angle experiments by Davies and West [21] indicated that the addition of sodium to the melt alters the interfacial energies at the growth front but that the interface profile is not affected by these changes. On the other hand the experiments demonstrated clearly that the growth rate of silicon in a eutectic melt is retarded by the addition of sodium. The authors concluded that

retardation of silicon growth by interfacial poisoning is the operative modification mechanism.

It has been shown [21, 35] that sodium addition reduces the diffusion rate of silicon in the melt but there is no positive evidence of a differential effect between silicon and aluminium. Sodium has no effect in modifying the untwinned pseudo-steady state growth at low interface velocities defined by Day and Hellawell [3] as region B. This appears to be conclusive evidence that a change in relative diffusion rates is not the operative mechanism of sodium modification. This objection does not apply to chill modification, where a change in relative diffusion rates with decreasing temperature is a highly probable cause of the reduction in lead distance which trips the transition.

Proposals (c) and (d) are closely related. In the discussion above of spheroidal primary silicon it was shown that poisoning of the twin-plane re-entrant edge by sodium results in relatively isotropic growth. Closer examination (Fig. 7) reveals that faceting is still pronounced, but with several crystallographic planes participating rather than {1 1 1} alone. It can be suggested that the impurity-induced flake–fibre transition results from very similar changes although faceted surfaces such as those in Fig. 7 have not yet been described for the eutectic fibres. We know [21] that sodium additions decrease the rate of growth of silicon in a eutectic melt. By analogy with the primary silicon behaviour we can expect that sodium rejected at the advancing interface will concentrate at the twin planes at the leading edges of the silicon flakes to produce the same effects as fast cooling. The TPRE advantage will be minimized and the lead distance S_β reduced. With sufficient sodium addition S_β can be reduced sufficiently to permit strongly coupled growth with a smooth interface profile to be established at very low interface velocities, probably down to about 4 μm sec^{-1} [3].

The simultaneous change to fibrous morphology must also be induced by the sodium. Davies and West [21] observed that the retardation due to sodium varied with crystallographic orientation. The appearance of facets other than {1 1 1} makes it fair to assume that this variation results in a trend to isotropic growth of the silicon. In other words, the effect of sodium is to reduce the faceted–non-faceted transition temperature as in (d) above, by selective adsorption on the faster-growing planes.

The reasoning above depends on separation of the transition mechanism into separate events which happen to coincide, but the coincidence is not improbable. The change to a smooth interface profile could be expected to occur quite sharply, at a critical interface velocity in chill modification or at a minimum solute content (also dependent on velocity) in impurity modification. In chill modification the critical velocity falls within the wide range of interface velocities over which the faceted–non-faceted progression occurs. It is thought to coincide with a stage at which surface facets have ceased to be obvious but at which growth flexibility is still limited by the faceting tendency. In impurity modification the fibrous morphology can be obtained at very slow interface velocities, e.g. 0.3 μm sec^{-1} [4] and if there is any separation between the two events it is unlikely to have been observed experimentally. It also seems unlikely that sodium addition would lead to completely isotropic growth of silicon at any undercooling, since its action is to adsorb on specific crystallographic planes. Hence the residual faceting tendency which forces a wide λ spacing in chill modifcation should also operate in impurity modification.

10. Conclusions

(1) The sodium distribution observed in spheroidal primary silicon crystals provides strong support for the concept that sodium rejected at an Al–Si eutectic growth front concentrates at twin plane re-entrant edges at the silicon growth tips and reduces or eliminates the growth rate advantage of the TPRE mechanism.

(2) The high twinning frequency of eutectic silicon is attributed to the attachment from the melt of silicon tetrahedra rather than single silicon atoms. The melt is said to contain a substantial proportion of silicon atoms bonded into tetrahedra and this proportion can be expected to increase as temperature falls.

(3) The flake–fibre transition is considered to depend on two events: (a) a reduction of the lead distance of silicon at the eutectic–liquid interface which leads to strongly coupled growth with a smooth solid–liquid interface; (b) a partial transition of the silicon phase from faceted towards non-faceted growth.

(4) In chill modification, produced by fast cooling, the most probable cause of the reduction in lead distance is a differential reduction in

diffusion rate of the two species in the eutectic melt, so that the potential growth rate of the aluminium phase decreases less rapidly with falling temperature than that of the silicon phase. At the same time the faceting tendency of silicon is reduced with increasing undercooling so that semi-isotropic fibrous growth is possible when the critical transition temperature range is reached.

(5) In impurity modification, due to sodium or strontium addition, it is proposed that the modifying agent removes the growth advantage of the TPRE mechanism by concentrating at the re-entrant edges and also reduces the anisotropic growth habit of silicon by adsorbing on specific crystallographic planes. In this way the agent operates to remove the silicon lead distance and to permit semi-isotropic fibrous growth similar to that observed in chill modification.

References

1. H. A. H. STEEN and A. HELLAWELL, *Acta Metall.* **20** (1972) 363.
2. D. C. JENKINSON and L. M. HOGAN, *J. Crystal Growth* **28** (1975) 171.
3. M. G. DAY and A. HELLAWELL, *Proc. R. Soc.* **305** (1968) 473.
4. H. FREDRIKSSON, M. HILLERT and N. LANGE, *J. Inst. Metals* **101** (1973) 285.
5. S. C. FLOOD and J. D. HUNT, *Metal Sci.* **15** (1981) 287.
6. A. HELLAWELL, *Prog. Mater. Sci.* 15 (1) (1970).
7. A. MOORE and R. ELLIOTT: ISI Pubn. 110, "Solidification of Metals" (Iron and Steel Institute, London, 1968) p. 167.
8. H. A. H. STEEN and A. HELLAWELL, *Acta Metall.* **23** (1975) 529.
9. A. J. McLEOD, L. M. HOGAN, C. M. ADAM and D. C. JENKINSON, *J. Crystal Growth* **19** (1973) 301.
10. C. B. KIM and R. W. HEINE, *J. Inst. Metals* **92** (1963–64) 367.
11. K. KOBAYASHI, P. H. SHINGU and R. OZAKI, *J. Mater. Sci.* **10** (1975) 290.
12. E. BILLIG, *Proc. R. Soc.* (*A*) **229** (1955) 346.
13. R. S. WAGNER, *Acta Metall.* 8 (1960) 57.
14. D. R. HAMILTON and R. G. SEIDENSTICKER, *J. Appl. Phys.* **31** (1960) 1165.
15. R. E. REED-HILL, "Physical Metallurgy Principles" (Van Nostrand, New York, 1964) p. 376.
16. A. A. CHERNOV, *J. Crystal Growth* **24/25** (1974) 11.
17. D. H. ST. JOHN and L. M. HOGAN, *ibid.* 46 (1979) 387.
18. V. DeL. DAVIES, *J. Inst. Metals* 93 (1964–5) 10.
19. K. KOBAYASHI and L. M. HOGAN, *Phil. Mag.* **40** (1979) 399.
20. S. INO, *J. Phys. Soc. Japan* **27** (1969) 941.
21. V. DeL. DAVIES and J. M. WEST, *J. Inst. Metals* **92** (1963–64) 175.
22. J. D. BERNAL, in "Liquids: Structure, Properties, Solid Interaction", edited by T. J. Hughel (Elsevier, New York, 1965) p. 25.
23. K. KOBAYASHI, P. H. SHINGU and R. OZAKI, in "Solidification and Casting of Metals" (Metals Society, London, 1979) p. 101.
24. E. M. PILARSKI, PhD thesis, University of Wisconsin, (1969).
25. B. TOULOUI and A. HELLAWELL, *Acta Metall.* **24** (1976) 565.
26. S. M. D. GLENISTER and R. ELLIOTT, *Metal Sci.* April (1981) 181.
27. R. ELLIOTT and S. M. D. GLENISTER, *Acta Metall.* **28** (1980) 1489.
28. R. ELLIOTT, "Eutectic solidifcation Processing" (Butterworths, London, 1983) p. 168.
29. R. M. JORDAN and J. D. HUNT, *Met. Trans.* **2** (1971) 3401.
30. *Idem, ibid.* 3 (1972) 1385.
31. M. SHAMUZZOHA and L. M. HOGAN, University of Queensland. Research in progress.
32. W. A. TILLER, in "Liquid Metals and Solidification" (American Society for Metals, Cleveland, 1958) p. 276.
33. C. W, HAWORTH and E. P. WHELAN, *J. Aust. Inst. Metals* **10** (1965) 184.
34. K. A. JACKSON, "Liquid metals and solidification" (American Society for Metals, Cleveland, Ohio, 1958) p. 174.
35. Y. TSUMURA, *Nippon Kinzoku Gakkai-Si* **21** (1957) 69.

Received 29 May
and accepted 3 July 1984